Water in the mantle: Results from electrical conductivity beneath the French Alps

Pascal Tarits, Sophie Hautot, F Perrier

Water in the mantle: Results from electrical conductivity beneath the French Alps

P. Tarits

UMR CNRS 'Domaines Océaniques', IUEM/UBO, Plouzané France

S. Hautot

School of Geosciences, Grant Institute, University of Edinburgh, Edinburgh, UK

F. Perrier

Service Radioanalyses, Chimie, Environnement, CEA, Bruyères-le-Châtel, France

Received 14 December 2003; revised 16 February 2004; accepted 23 February 2004; published 20 March 2004.

[1] A deep magnetotelluric sounding in the French Alps provided a vertical electrical conductivity profile between ~200–1000 km. Two prominent features are observed. First, the conductivity in the depth range 400–800 km is smaller than the conductivity of a pyrolite mantle obtained from laboratory results for a normal geotherm. Second, the data do not require the conductivity to change throughout the transition zone (410–660 km). In this part of the mantle, a temperature of 350–450 C less than normal explains the magnetotelluric conductivity profile. At 200–400 km, our model favors a cold mantle with 1000–1500 ppm of water dissolved in olivine. If correct, this model suggests that the subducted slab is dehydrated before reaching the transition zone. *INDEX TERMS:* 1515 Geomagnetism and Paleomagnetism: Geomagnetic induction; 3914 Mineral Physics: Electrical properties; 7218 Seismology: Lithosphere and upper mantle; 8120 Tectonophysics: Dynamics of lithosphere and mantle—general. **Citation:** Tarits, P., S. Hautot, and F. Perrier (2004), Water in the mantle: Results from electrical conductivity beneath the French Alps, *Geophys. Res. Lett.*, *31*, L06612, doi:10.1029/2003GL019277.

1. Introduction

[2] Water is a minor phase but plays an important role in a number of processes in the mantle. The study of the water content in MORB suggests 100–500 ppm in the bulk mantle. In subduction zone, dehydration of hydrous minerals carried by the subducted lithosphere may be responsible for large amount of water in the mantle. Whether this water is transported deep in the mantle is a key question to quantify the mass balance of water between the upper and lower mantle and to determine its recycling time [e.g., *Angel et al.*, 2001]. Most of the results are from laboratory studies as the detection of water in the deep mantle is difficult with geophysical techniques.

[3] Water seems to have a strong influence on mantle electrical conductivity even in very small quantity (a few 100 ppm) [*Karato*, 1990]. Conductivity models accounting for water dissolution in silicate [*Karato*, 1990] or free water [*Tarits*, 1986] may explain the difference between conductivity obtained from induction data and conductivity measured for dry minerals. At depths larger than 200 km, the solubility of hydrogen in olivine and in its high pressure phases suggests that free water is unlikely. Hydrogen diffusion then could be the factor controlling the electrical conductivity in the upper mantle. As a result, the knowledge of electrical conductivity versus depth obtained from deep magneto-telluric (MT) techniques may provide insight on the amount of water in the mantle [e.g., *Hirth et al.*, 2000]. Water also depresses the solidus of mantle minerals and may trigger partial fusion deep in depth, also increasing conductivity significantly [e.g., *Shankland and Waff*, 1977].

[4] Here we present a deep MT sounding realized in the French Alps, from which mantle conductivity values down to ~1000 km were obtained. The site (SURF) is located in the Western Alps orogene (Figure 1). The Western Alps results from the Europe-Africa collision. Subduction seems to play a central role to control the Western and Central Europe mantle dynamics. Recent tomography results suggest blockage of subducted slabs at the 660 km seismic discontinuity with fast material in the transition zone (TZ, 410–660 km) [*Wortel and Spakman*, 2000; *Piromallo and Morelli*, 2003]. Subduction zones are associated with low temperature in the mantle as well as hydration/dehydration reactions. Consequently, Western and Central Europe subduction should control the mantle conductivity beneath SURF.

2. The Experiment

[5] SURF (Figure 1) is on a topographic ridge, the Sur-Frêtes ridge, which separates two artificial lakes whose water levels vary on a yearly cycle, inducing hydrological and mechanical stress on the ridge. An array of 14 electrical measurements points [*Trique et al.*, 2002] was set across the Sur-Frêtes ridge. The electrical potential differences were measured at 20 dipoles. The three components of the magnetic field were also recorded with a fluxgate magnetometer installed on the top of the ridge. The electrical and magnetic data were measured continuously from November 1995 to December 1998.

[6] The magnetotelluric transfer function (MTF) between each electrical dipole and the magnetic field variations (periods from 870–72,000 s) has been determined by S. Hautot (Temporal variations of large sale telluric distorsion associated with ground water flow, submitted to *Earth and*

0094-8276/04/2003GL019277

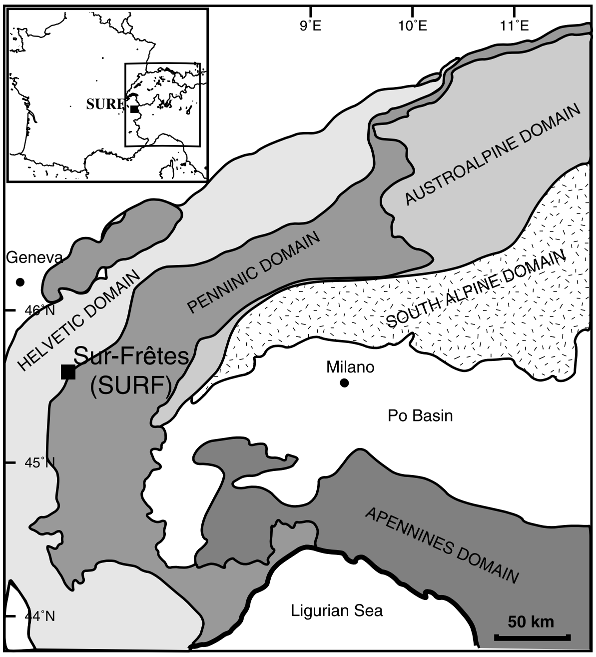

Figure 1. Simplified geodynamic map of the Western Alps.

Planetary Science Letters, 2003, hereinafter referred to as Hautot, submitted manuscript, 2003). For each dipole E of azimuth θ, the MTF components $Z_{\theta x}$ and $Z_{\theta y}$ were obtained using the relation $E_\theta = Z_{\theta x}B_x + Z_{\theta y}B_y$ where B is the magnetic field in the North (x) and in the East (y) directions. The values $Z_{\theta x}$ and $Z_{\theta y}$ are a linear combination of the four MTF coefficients Z_{xx}, Z_{xy}, Z_{yx}, Z_{yy}, cosθ and sinθ. Solving the system $(Z_{\theta ix}, Z_{\theta iy}) = F_i(Z_{xx}, Z_{xy}, Z_{yx}, Z_{yy})$ with $i = 1–20$ gives the four MTF coefficients. The direction of maximum (Z_1) and minimum (Z_2) values of MTF were obtained from the tensor decomposition approach proposed by *Counil et al.* [1986].

[7] The direction found (35°N) is frequency independent and well correlated to the geology trend (Figure 1). The coefficients Z_1 and Z_2 are presented in Figure 2. The parallel moduli and the identical phases over most of the period range are typical of static shift (SS) (Hautot, submitted manuscript, 2003). Local induction affects the phase of Z_2 below ∼4000 s. SS is caused by electric charge accumulation at contrasts or gradients of electrical conductivity which distort locally without dephasing the electric field induced at regional scale [*Le Mouel and Menvielle*, 1982]. The source of SS at SURF is local (Hautot, submitted manuscript, 2003) (km-scale) compared to the scale of the induced field (100 km or more). The data in Figure 2 may be accounted for with the super-imposition of a mean 1-D field E_n induced regionally and a locally distorted field proportional to the former through a real constant.

[8] The real coefficients between the 1-D MTF Z_n and Z_1, Z_2 were determined using the geomagnetic variation field, which is insensitive to SS. At periods over several hours, an equivalent 1-D MTF was derived in the frequency domain from the ratio $R = B_z/H$ of the vertical component B_z to the horizontal component in the magnetic North H. The ratio R may be used to derive magnetic transfer functions at periods from less than a day to a few years [*Banks*, 1969]. The ratio R at SURF was obtained at periods 40,000–430,000 s and was converted into a magnetic MTF Z_n (Figure 2). At 1 day period and below, the phase value is biased upward because of the daily variation while the modulus is not (Figure 2).

[9] The SS factor was obtained from the magnetic $|Z_n|$ (Figure 2) at periods common with $|Z_1|$ and used to correct it at all other periods. The final Z_n is shown in Figure 2. Different tests can be used to demonstrate the one-dimensionality of Z_n. The algorithm D^+ [*Parker*, 1980] was used here. It provides the absolute minimum misfit and the maximum depth of resolution (∼900–1000 km) for a theoretical earth comprised of alternance of highly resistive layers and thin slabs of high conductance. The rms found (0.55) is fairly homogeneously distributed over all periods. The value less than 1 indicates that the error bars are slightly overestimated.

3. Conductivity Models

[10] A difficulty in data inversion is the choice of parameterisation of the earth. Induction theory tells us that the inversion of a perfect 1-D MTF leads to a unique conductivity profile [*Bailey*, 1970], a rare situation in inverse problem theory. Limited frequency sampling of noisy data leads us to the more common case of infinite number of solutions. Here we restricted our analysis to two classes of models, namely layered models and smooth models. The reason for using smooth models is to obtain structures with minimum features required by the data. Layered models minimize the number of parameters and here they take explicitly into account the major mineral and/or chemical transitions in the mantle. Data inversion was carried out with a non-linear Bayesian approach [*Tarits et al.*, 1994; *Grandis et al.*, 1999].

[11] The SURF layered model in Figure 3 corresponds to a misfit to the data of *rms* = 0.68. A maximum of 4 layers was required by the data. The conductivity increases with depth with rapid changes at ∼240, ∼640 and, ∼800 km. The a posteriori law obtained from the Bayesian inversion for each parameter (conductivity and depth) is a function of all other parameters [*Tarits et al.*, 1994]. Hence it takes into account the trade-off between resolution on conductivity and resolution on layer thickness, leading to large uncertainties in the depth range 600–800 km. The smooth Bayesian inversion [*Grandis et al.*, 1999] of the same data set leads to models with misfit ranging from *rms* = 0.73–0.84 depending on the degree of smoothness. The smooth conductivity profile has inflexions at ∼250 km and ∼500 km. The conductivity increases monotically down

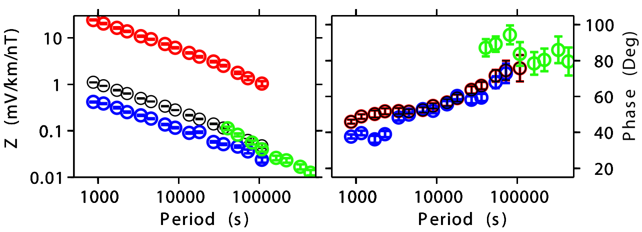

Figure 2. MT transfer function obtained in SURF. Z_1 and Z_2 values (amplitude and phase) are in red and blue respectively. Magnetic Z_n is green. The static shift corrected MTF Z_n is black. Error bars are one standard deviation.

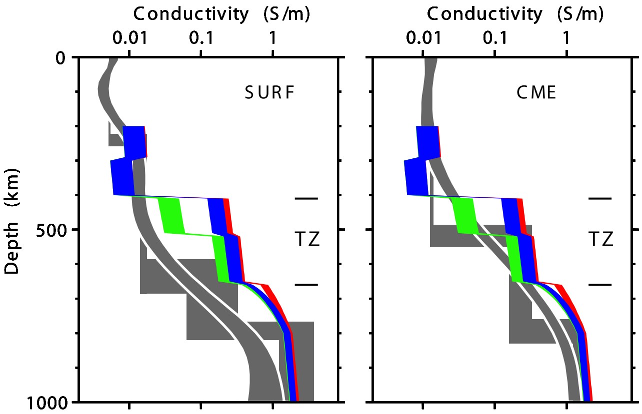

Figure 3. Sur-Frêtes (SURF) and Europe (CME) conductivity profiles. The smooth and the layered best fitting conductivity models of width equal to ±1 standard deviation are in grey. Laboratory conductivity values for the LCM are from *Xu et al.* [2000]. They are presented here for two different mixing laws, the Hashin-Shtrikman lower (HS^{-}, green) and upper (HS^{+}, red) bounds and the Effective Medium (EM, blue) value (see *Xu et al.* [2000] for details). The values were calculated at ±50 C for the normal geotherm shown in Figure 4.

to 800–900 km. It averages out the steps observed in the layered model and reaches a value slightly less than for the layered model below 800–900 km (Figure 3). This discrepancy can be attributed to the limited depth resolution of SURF data.

[12] The SURF conductivity profile is compared with the mean conductivity model for Europe (CME) proposed by *Olsen* [1998]. In order to compare SURF to CME in a consistent way, we re-analysed Olsen's data with the approach used for SURF. The layered and the smooth conductivity models are presented in Figure 3. They are similar to the original layered and smooth models obtained by *Olsen* [1998]. Both smooth and layered CMEs show that conductivity increases by 2 orders of magnitude between 200–800 km. Conductivity is poorly resolved in the depth range 200–400 km. The layered CME has a large discontinuity in the middle of the transition zone (~500 km) rather than at its top or bottom. There is no clear discontinuity near 660 km while the 800 km deep conductivity change is apparent. The smooth model averages out the 500 km discontinuity. Both layered and smooth models agree below ~800 km.

[13] *Xu et al.* [2000] compiled laboratory conductivity data to obtain an experimental conductivity model (LCM, Figure 3) for the Earth mantle. The model takes into account the petrology and the thermodynamics of the mantle for different mixing laws but does not explicitly include water or partial melting. This laboratory model as well as others [e.g., *Farber et al.*, 2000] shows that conductivity increases by 1 or 2 order of magnitude in the TZ with or without a large discontinuity at 520 km depending on the conductivity models (Figure 3). *Xu et al.* [2000] assume dry condition throughout the TZ and attribute the increase in conductivity to the phase transformations. *Nishihara et al.* [2003] show that water may have dissolved in the silicate compound during the experiment which would imply that the wadsleyite is under wet condition and the conductivity enhanced by hydrogen diffusion. The LCM is discontinuous at the bottom of the TZ. Then the conductivity increases regularly below with a change in slope at ~800 km. This feature may correspond to the limit below which Al-bearing perovskite controls the lower mantle conductivity [*Xu et al.*, 2000].

[14] LCM appears to agree with SURF conductivity above ~300 km and below ~800 km for the layered model (Figure 3). Near and within the TZ the SURF data do not require the conductivity to change, in contrast with LCM (Figure 3). The SURF model is more resistive than LCM between 400–800 km. LCM agrees reasonably well with the layered CME (Figure 3) above 660 km. The discontinuity predicted by laboratory results at the top of the TZ is observed within the TZ (~500 km). The HS^{-} bound fits LCM best between 400–500 km (Figure 3). This bound corresponds to conductivity controlled by clinopyroxene [*Xu et al.*, 2000].

[15] The ~800 km conductivity change is present both locally at SURF and regionally in CME. The layered SURF model and both layered and smooth CMEs have the same conductivity value at that depth (~1 S/m) in agreement with laboratory data. LCM is in fair agreement with the smooth CME below 660 km. The conductivity averaged over Europe in the depth range 200–1000 km is therefore reasonably well explained by LCM. The slightly higher conductivity between 300–400 km in CME compared to LCM may be accounted for with hydrogen diffusion in olivine [*Karato*, 1990]. Consequently, LCM may be a good petrological and thermodynamical model to analyse the conductivity profile at SURF.

4. Discussion

[16] The SURF conductivity model has two prominent features. First, the conductivity below ~400 km is less than LCM (Figure 3) by up to one order of magnitude down to ~800 km. Second, there is no discontinuity required by the data at the TZ.

[17] For a given petrological model for the mantle, water content and temperature control the conductivity values. Because LCM in the TZ seems to correspond to wet condition [*Nishihara et al.*, 2003], which could explain the conductivity enhancement observed through the TZ, we may question whether there is any significant conductivity change at the 410 km and 520 km discontinuity under dry or water-poor condition. The conductivity of a water depleted upper mantle would then be fairly uniform. This result would be in agreement with the upper mantle SURF conductivity data. New laboratory data on conductivity of TZ minerals under well controlled water content are needed to test this model.

[18] The agreement between LCM and CME in the TZ (Figure 3) suggests that on average the TZ may have the water content found by *Nishihara et al.* [2003]. If the TZ beneath SURF was not water depleted, then a decrease of 350–450 C in temperature compared with the normal geotherm would produce a LCM which explains well the SURF conductivity in the TZ and below (Figure 4). Temperature

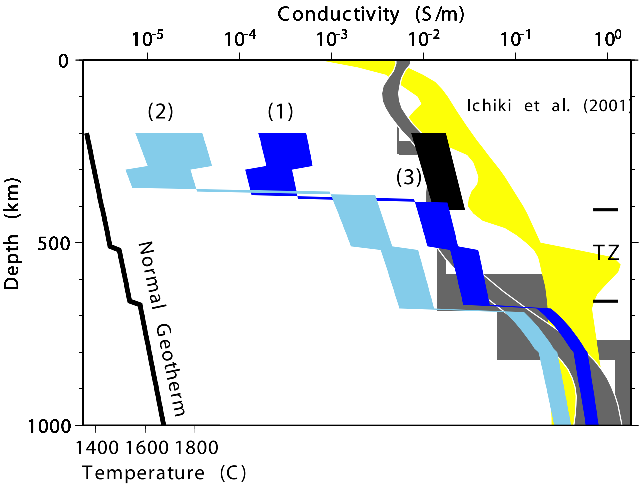

Figure 4. SURF conductivity profile compared with LCM re-calculated for temperatures 350–450 C (1) and 550–650 C (2) less than the normal geotherm. (3) Conductivity of isotropic olivine with 1200 ppm of water calculated as by *Karato* [1990] for a temperature ±50 C of the normal geotherm above the TZ. *Ichiki et al.* [2001] conductivity model is shown for comparison.

differences between a cold subducted slab and the surrounding mantle at the depth of the TZ could be locally as much as ~600 C [*Collier et al.*, 2001]. For temperature differences of 550–650 C, the TZ LCM values are smaller than SURF values (Figure 4) which would require an additional conductive phase, probably water to explain SURF. A ~600 C difference in the TZ at the scale of the Western and Central Alps may be too large for subducted material accumulating since as early as Oligocene and would make the seismic velocity too fast [*Piromallo and Morelli*, 2003]. The SURF conductivity values in TZ are in contrast with *Ichiki et al.* [2001] results (Figure 4) beneath northeastern China where high conductivity observed in the TZ might be associated with water released from a stagnant slab. These observations suggest that there are more than one process associated with hydration and dehydration of the upper mantle. Low temperatures seem to persist in the upper part of the lower mantle above 800 km according to the low SURF conductivity values (Figure 3). Again 350–450 C temperature differences compared with the normal geotherm explains well the SURF conductivity values (Figure 4). At greater depth, conductivity is not resolved well enough to discuss the temperature.

[19] Above TZ, SURF conductivity values are close to CME and slightly higher than LCM (Figure 3). For a normal geotherm, a few 100 ppm of water dissolved in olivine would explain the conductivity value [*Hirth et al.*, 2000]. According to *Piromallo and Morelli* [2003], the mantle beneath SURF is fast, suggesting a temperature colder than normal. For the temperature difference obtained in the TZ (350–450 C), the LCM conductivity is much less than observed (Figure 4) implying the existence of a conductive phase. This phase is unlikely to be partial melting because the temperature (1000–1100 C) would be less than the wet solidus in this depth range. Water is a good candidate and may come from the dehydration of the subducting slab. Water may dissolve into olivine in the subducting lithosphere and in the surrounding mantle, thus enhancing the conductivity. The amount of water (1000–1500 ppm) needed to explain the SURF conductivity value (Figure 4) is obtained from hydrogen diffusion in olivine [*Karato*, 1990] and is in agreement with dehydration results from *Schmidt and Poli* [1998].

[20] If our interpretation was correct, it is coincidental that conductivity values above and below the 410 km phase transition are close. Given the uncertainty in our model, a discontinuity is not excluded but seems to be too small to be resolved by the induction data. A conductivity profile uniform throughout the upper mantle could also be the result of a water depleted TZ.

[21] In summary, the deep conductivity profile obtained beneath the Western Alps in the depth range 200–1000 km with laboratory studies agrees with a cold mantle where water has been extracted from the subducted slabs above the TZ and possibly dissolved in mantle olivine. In the TZ and in the uppermost lower mantle, the data would agree with cold mantle material.

[22] **Acknowledgments.** We thank Michel Menvielle for providing the smooth Bayesian inversion code and an anonymous reviewer for very helpful comments.

References

Angel, R. J., D. J. Frost, N. L. Ross, and R. Hemley (2001), Stabilities and equations of state of dense hydrous magnesium silicates, *Phys. Earth Planet. Int.*, *127*, 181–196.
Bailey, R. C. (1970), Inversion of the geomagnetic induction problem, *Proc. R. Soc. London*, *315*, 185–194.
Banks, R. (1969), Geomagnetic variations and the electrical conductivity of the upper mantle, *Geophys. J. R. Astron. Soc.*, *17*, 457–487.
Collier, J. D., G. R. Helffrich, and B. J. Wood (2001), Seismic discontinuities and subduction zones, *Phys. Earth Planet. Int.*, *127*, 35–49.
Counil, J. L., M. Menvielle, and J. L. Le Mouel (1986), Associate and conjugate direction concepts in magnetotellurics, *Ann. Geophys.*, *4*, 115–130.
Farber, D. L., Q. Williams, and F. J. Ryerson (2000), Divalent cation diffusion in Mg_2SiO_4 spinel (ringwoodite), β phase (wadleysite), and olivine: Implications for the electrical conductivity of the mantle, *J. Geophys. Res.*, *105*, 513–529.
Grandis, H., M. Menvielle, and M. Roussignol (1999), Bayesian inversion with Markov chains-I. The magnetotelluric one-dimensional case, *Geophys. J. Int.*, *138*, 757–768.
Hirth, G., R. L. Evans, and A. D. Chave (2000), Comparison of continental and oceanic mantle electrical conductivity: Is the archean lithosphere dry?, *Geochim. Geophys. Geosyst.*, *1*, 2000GC000048.
Ichiki, M., M. Uyeshima, H. Utada, Z. Guoze, T. Ji, and M. Mingzhi (2001), Upper mantle conductivity structure of the back-arc regoin beneath northeastern China, *Geophys. Res. Lett.*, *28*, 3773–3776.
Karato, S. (1990), The role of hydrogen in the electrical conductivity of the upper mantle, *Nature*, *347*, 272–273.
Le Mouel, J. L., and M. Menvielle (1982), Geomagnetic variation anomalies and deflection of telluric currents, *Geophys. J. R. Astron. Soc.*, *68*, 575–587.
Nishihara, Y., T. Shinmei, and S. Karato (2003), Kinetics of grain-growth in wasdleyite: Implications for point defects chemistry, Eos Trans, *American Geophysical Union*, *84*(46), Fall Meet. Suppl., T11C-0397.
Olsen, N. (1998), The electrical conductivity of the mantle beneath Europe derived from C-responses from 3 to 720 hr, *Geophys. J. Int.*, *133*, 298–308.
Parker, R. L. (1980), The inverse problem of electromagnetic induction: Existence and construction of solutions based on incomplete data, *J. Geophys. Res.*, *85*, 4421–4428.
Piromallo, C., and A. Morelli (2003), P wave tomography of the mantle under the Alpine-Mediterranean area, *J. Geophys. Res.*, *108*(B2), 2065, doi:10.1029/2002JB001757.
Schmidt, M. W., and S. Poli (1998), Experimentally based water budgets for dehydrating slabs and consequences for arc magma generation, *Earth Planet. Sci. Let.*, *163*, 361–379.

Shankland, T. J., and H. S. Waff (1977), Partial melting and electrical conductivity anomalies in the upper mantle, *J. Geophys. Res.*, *82*, 5409–5416.

Tarits, P. (1986), Conductivity and fluids in the cceanic upper mantle, *Phys. Earth Planet. Int.*, *42*, 215–226.

Tarits, P., V. Jouanne, M. Menvielle, and M. Roussignol (1994), Bayesian sstatistics of non-linear inverse problems: Example of the magnetotelluric 1-D inverse problem, *Geophys. J. Int.*, *119*, 353–368.

Trique, M., F. Perrier, T. Froidefond, and J. P. Avouac (2002), Fluid flow near reservoir lakes inferred from the spatial and temporal analysis of the electric potentiel, *J. Geophys. Res.*, *107*(B10), 2239, doi:10.1029/2001JB000482.

Wortel, M. J. R., and W. Spakman (2000), Subduction and slab detachement in the mediterranean-carpathian region, *Nature*, *290*, 1910–1917.

Xu, Y., T. J. Shankland, and B. T. Poe (2000), Laboratory-based electrical conductivity in the Earth's mantle, *J. Geophys. Res.*, *105*, 27,865–27,875.

S. Hautot, School of Geosciences, Grant Institute, University of Edinburgh, West Mains Road, Edinburgh EH9 3JW, UK. (shautot@glg.ed.ac.uk)

F. Perrier, Service Radioanalyses, Chimie, Environnement, CEA, BP12, 91680 Bruyères-le-Châtel, France. (frederic.perrier@cea.fr)

P. Tarits, IUEM, UMR 'Domaines Océaniques', Place Nicolas Copernic, F-29280 Plouzané, France. (tarits@univ-brest.fr)